Vascular endothelial cell–specific phosphotyrosine phosphatase (VE-PTP) activity is required for blood vessel development

Sebastian Bäumer, Linda Keller, Astrid Holtmann, Ruth Funke, Benjamin August, Alexander Gamp, Hartwig Wolburg, Karen Wolburg-Buchholz, Urban Deutsch, and Dietmar Vestweber

VE-PTP, a receptor-type phosphotyrosine phosphatase, associates with the tyrosine kinase receptor Tie-2 and VE-cadherin and enhances the adhesive function of the latter. Here, VE-PTP was found to be restricted to endothelial cells, with a preference for arterial endothelium. Mutant mice expressing a truncated, secreted form of VE-PTP lacking the cytoplasmic and transmembrane domains and the most membrane-proximal extracellular fibronectin type III repeat, showed severe vascular malformations causing lethality at 10 days of gestation. Although blood vessels were initially formed, the intraembryonic vascular system soon deteriorated. Blood vessels in the yolk sac developed into dramatically enlarged cavities. In explant cultures of mutant allantoides, endothelial cells were found next to vessel structures growing as cell layers. No signs for enhanced endothelial apoptosis or proliferation were observed. Thus, the activity of VE-PTP is not required for the initial formation of blood vessels, yet it is essential for their maintenance and remodeling. (Blood. 2006;107: 4754-4762)

Introduction

The formation of nascent blood vessels during embryonic development requires several cell surface receptors as well as cell adhesion molecules. Initially, a primitive vascular plexus is formed, which becomes remodeled and matures by recruiting perivascular cells.[1-4] The vascular endothelial growth factors (VEGFs) and their receptors, of which VEGFR-2 is instrumental for vasculogenesis, the formation of primary vascular plexus,[5] are among the factors and receptors known today to be essential for the development of the vasculature. The Tie-2 receptor and its ligands, the angiopoietins, are involved in blood vessel sprouting, remodeling, and integrity. Various EphB receptors and ephrin-B ligands participate in establishing the primary vessel architecture and in vessel maturation, while the recruitment of pericytes to the newly formed vessels requires PDGF-B and its receptor PDGFR β. A cell adhesion molecule of dominant importance for endothelial cell contacts is the endothelial-specific cadherin, VE-cadherin, which was shown to be essential for the formation of a stable blood vessel system and thus embryonic development.[6,7] Surprisingly, VE-cadherin was indeed dispensable for initial vessel formation, yet was required for their maintenance.[8]

Several of the most important receptors in angiogenesis are tyrosine kinases that are prominently and often quite selectively expressed in endothelial cells. In contrast, much less is known about the role of receptor-type tyrosine phosphatases during blood vessel development. In general, the gene disruption approach was unable to reveal the physiologic functions for several RPTPs,[9] yet was fruitful for several RPTPs that play roles in the adult neuronal system. For the vascular system, RPTPμ was found to participate in the flow-induced dilation of mesenteric resistance arteries[10]; however, it was not essential for embryonal development. Density-enhanced phosphatase 1 (DEP-1, CD148), although not restricted to endothelial cells, is the only RPTP for which a function in angiogenesis has been reported.[11] Mice harboring a *DEP-1* mutant allele died before embryonic day 11.5 with disorganized vascular structures.

Vascular endothelial receptor tyrosine phosphatase (VE-PTP) is the only known RPTP specifically expressed in endothelial cells, as had been shown by in situ hybridizations of embryonal mouse tissues.[12] In addition, the same report demonstrated that VE-PTP associates with the tyrosine kinase Tie-2 in transfected COS cells, causing its dephosphorylation. VE-PTP represents the mouse homolog of human HPTP-β.[13] Recently, we showed that VE-PTP is associated with VE-cadherin in endothelial cells, an association that requires the extracellular parts of each protein.[14] Analyzing the consequences of this interaction, we found that inducing VE-PTP expression in transfected cells, using a suitable inducible promoter, increased the adhesive function of VE-cadherin and concomitantly decreased its tyrosine phosphorylation level.

The endothelial selective expression of VE-PTP in the embryo and the association of VE-PTP with 2 endothelial cell-surface proteins essential for embryonal development and angiogenesis prompted us to analyze the physiologic function of this phosphatase. We

From the Max-Planck-Institute of Molecular Biomedicine, Münster, Germany; the Theodor-Kocher-Institute, University of Bern, Switzerland; and the Institute of Pathology, University of Tübingen, Germany.

Submitted January 12, 2006; accepted February 15, 2006. Prepublished online as *Blood* First Edition Paper, March 2, 2006; DOI 10.1182/blood-2006-01-0141.

Supported by funding through the DFG (SFB629) and the Max-Planck-Society to D.V.

S.B., L.K., A.H., R.F., B.A., A.G., H.W., and K.W.-B. performed, designed, and analyzed experiments; S.B. and L.K. contributed to writing the paper; U.D. and D.V. initiated the study, designed and supervised the research project, contributed to data analysis and interpretation, and wrote the paper.

The online version of this article contains a data supplement.

An Inside *Blood* analysis of this article appears at the front of this issue.

Reprints: Dietmar Vestweber, Max-Planck-Institute of Molecular Biomedicine, Von-Esmarch-Str 56, D-48149 Münster, Germany; e-mail: vestweb@uni-muenster.de; or Urban Deutsch, Theodor-Kocher-Institute, University of Bern, Freiestr 1, CH-3012 Bern, Switzerland; e-mail: urban.deutsch@tki.unibe.ch.

The publication costs of this article were defrayed in part by page charge payment. Therefore, and solely to indicate this fact, this article is hereby marked "advertisement" in accordance with 18 U.S.C. section 1734.

found that VE-PTP is indeed exclusively expressed on endothelial cells, based on immunohistochemistry of adult and embryonal tissues. Mice carrying a gene disruption leading to the expression of a truncated, secreted form of VE-PTP lacking the complete intracellular and transmembrane domains and the most membrane-proximal extracellular domain were embryonic lethal and showed severe vascular defects in extraembryonic and intraembryonic tissues.

Materials and methods

Mice

The VE-PTP mutant mouse strain T741 was purchased from Deltagen (Redwood City, CA). The targeting construct was created by homologous recombination in *Escherichia coli.* Modified BAC DNA was electroporated into embryonic stem cells; clones were selected with G418, screened by genomic polymerase chain reaction (PCR), and injected into C57BL/6 blastocysts that were then transferred to foster mice. Chimeric mice were mated to C57BL/6 females to score for germ-line transmission. VE-PTP mutant mice were backcrossed to C57Bl/6 mice for at least 8 generations. Flk-1–deficient mice were a gift from Janet Rossant (Hospital for Sick Children, and Department of Medical Genetics and Microbiology, University of Toronto, Toronto, ON, Canada)[15]; Tie-2–deficient mice were provided by Daniel Dumont (Sunnybrook and Women's Research Institute, Toronto, ON, Canada).[16] For timed matings, mice were mated for 3 hours. Embryos (E8.5-E16.0) were routinely checked for heartbeat before analysis.

Genotyping

VE-PTP–specific genotyping was performed by multiplex PCR using tail or yolk sac lysates as a template. Primers were (A) forward, 5′-GCATCTTTT-GAGATCGCAGGATCTG-3′ (endogenous); (B) reverse, 5′-GGGTGGGAT-TAGATAAATGCCTGCTCT-3′ (insertion-cassette specific); and (C) reverse, 5′-GTGTCTGTACTCCAGGTAGGAAGGG-3′ (endogenous). The sizes of the amplified fragments were as follows: (A + B) 420 bp, (A + C) 204 bp.

Immunoblotting, immunoprecipitation, and flow cytometry

Immunoblotting, immunoprecipitations, and flow cytometry were done as described before.[14] The apparent molecular weight (MW) of VE-PTP was re-estimated using an MW marker kit containing markers up to 500 kDa (High Mark; Invitrogen, Karlsruhe, Germany), resulting in the determination of a considerably higher apparent MW than had been determined before. For blots, samples were immunoprecipitated with polyclonal VE-PTP-C antibodies and analyzed after transfer with 1 μg/mL monoclonal antibody (mAb) 109.3. Immunoprecipitations were performed with endothelioma cells metabolically labeled with [^{35}S]methionine/cysteine (0.2 mCi/mL, Promix; Amersham Biosciences, Munich, Germany) for 16 hours. For each immunoprecipitation, 3 μg affinity-purified antibodies bound to γ-bind-Sepharose (Amersham Biosciences) was used. For fluorescence-activated cell sorter (FACS) analysis, cells were incubated with 10 μg/mL mAb.

Generation of endothelioma cell lines

Polyoma middle T immortalization of endothelial cells was carried out as described[17] starting from E9.5 mouse embryos.

Antibodies

The following mAbs against mouse antigens (in parentheses) were used: MEC13.3 (PECAM-1) and 3C4 (ICAM-2), both from BD/Pharmingen (Heidelberg, Germany); 11D4.1 (VE-cadherin)[18] and VE1.1 (VE-cadherin) (Ulrike Samulowitz and D.V., manuscript in preparation); MJ7/18 (endoglin; American Type Culture Collection, Rockville, MD); 3G1 (Tie-2)[19]; AVAS-12 (VEGFR-2),[20] a gift from Dr Shin-Ichi Nishikawa (Laboratory for Stem Cell Biology, RIKEN Center for Developmental Biology, Kobe, Japan); 7C7.1 (endomucin)[21]; N-cad 7 and 8 (N-cadherin) (B.A., S.B., and D.V., manuscript in preparation); mAb 9661 (caspase 3) from Cell Signaling Technology (Danvers, MA); and mAb 07-679 (phosphohistone-3) from Upstate (Dundee, United Kingdom). Monoclonal antibodies against mouse VE-PTP were generated by immunizing rats with a VE-PTP-Fc fusion protein. Immunization, hybridoma-fusion, and screening were done as described.[18,22] Of 16 isolated clones reacting with VE-PTP, mAb 109.3 (IgG2a) and mAb 85.1 (IgG1) were used in the present study.

VE-PTP-Fc fusion protein

The fusion protein was constructed such that the first 8 fibronectin type III–like repeats ending with the amino acid proline at position 732 of VE-PTP were fused in frame with the Fc part of human IgG1 (starting with amino acid proline at position 239). This construct cloned into pcDNA3 (Invitrogen) was stably transfected into CHO cells, and the fusion protein was purified by protein A Sepharose affinity purification as described.[23]

Histochemical detection of β-galactosidase activity

Dissected embryos were fixed in cold 4% paraformaldehyde/PBS for 10 minutes and rinsed twice with PBS, and whole mounts were stained overnight in X-Gal buffer (0.1 M ferricyanide, 0.1 M ferrocyanide, 4 mM KCl, 1 mg/mL X-Gal in PBS at 37°C). After subsequent washing in PBS, specimens were cleared in glycerol and photographed using a Zeiss (Göttingen, Germany) Stemi SV11 stereomicroscope in conjunction with a Nikon (Düsseldorf, Germany) D100 digital camera.

Immunolabeling techniques

Whole-mount stainings of embryos and immunohistology of cryostat and paraffin sections as well as TUNEL staining were done as described.[24] For the analysis of immunofluorescence-labeled yolk sac whole mounts, yolk sacs were removed from the embryo after the staining process and attached to poly-L-lysine–coated glass slides (Menzel-Gläser, Nußloch, Germany). They were examined with a Zeiss Axioskop 2 fluorescence microscope in conjunction with a Diagnostic Instruments RT KE/SE Spot digital camera (Sterling Heights, MI).

Allantois culture and immunolabeling

Allantoides were dissected from E8.0 to E8.5 embryos, cultured for 22 hours, and fixed as described.[25] Immunostaining was done as described.[25] For blocking of VE-cadherin, allantoides were cultured in the presence of 25 μg/mL mAb VE1.1 or an IgG2a isotype control antibody. For laser scanning confocal microscopy of cultured allantoides, immunolabeled explants were examined with a TCS confocal microscope and imaging system (Leica, Bensheim, Germany). Optical sections of the cultured explants were collected along the z-axis and collapsed into a single focal plane using the manufacturer's software. Computer-assisted quantification of PECAM-1 staining was achieved with a stereomicroscope and camera (see "Immunolabeling techniques") using Adobe Photoshop 7.0 software (Adobe Systems, San Jose, CA).

Electron microscopy

Electron microscopy was done as described.[24] A Zeiss EM 10 microscope (Zeiss, Oberkochen, Germany) was used.

Results

Analysis of VE-PTP mutant mice

Mutation of the *VE-PTP* gene was achieved by insertion of a promoter-less IRES-lacZ-pgk-neo cassette into the VE-PTP gene locus and thus replacing a 3.6-kb genomic sequence of the *VE-PTP* gene starting within exon 17 and ending in exon 19. This insertion

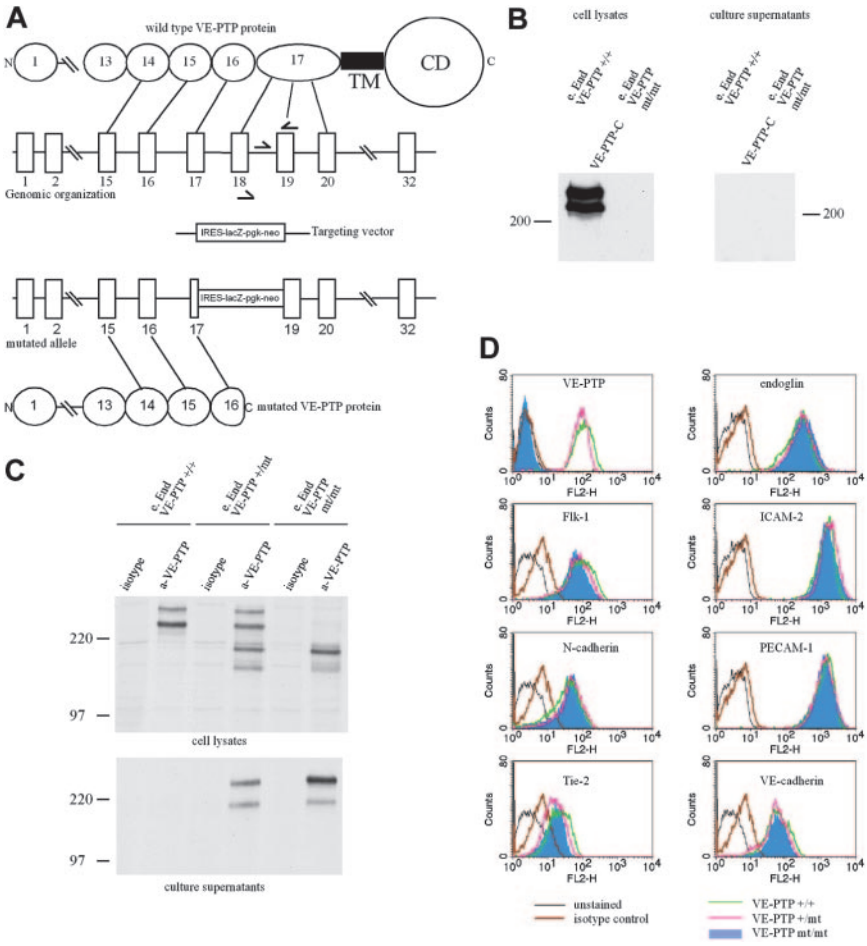

Figure 1. Targeted disruption of the mouse VE-PTP gene. (A) Targeting strategy. An IRES-lacZ-pgk-neo cassette was inserted between VE-PTP exons 17 and 19, resulting in a truncated protein lacking the transmembrane, the cytoplasmic, and the 17th extracellular domains. Exons are given as open rectangles; arrows depict the location of primers for genotyping; CD indicates cytoplasmic domain; and TM indicates transmembrane domain. Drawing is not to scale. (B) Western blot analysis of cell lysates and culture supernatants (as indicated) from embryonic endothelioma cells established from wild-type (VE-PTP$^{+/+}$) and homozygous (VE-PTP$^{mt/mt}$) VE-PTP mutant embryos. Blots were analyzed with a polyclonal serum against the C-terminus of VE-PTP (VE-PTP-C). (C) Autoradiograph of VE-PTP immunoprecipitations of embryonic endothelioma cells established from wt, heterozygous, or homozygous VE-PTP mutant embryos (as indicated), metabolically labeled with [^{35}S]-methionine/cysteine. Wild-type and truncated mutant forms of VE-PTP were immunoprecipitated with mAb 109.3 directed against the extracellular domain of VE-PTP. (D) FACS analysis showing the surface expression of major endothelial marker proteins of endothelioma cells of wild-type, heterozygous, and homozygous VE-PTP mutant phenotype. Note that homozygous mutant endothelioma cells showed no FACS signal for VE-PTP. Mutation of VE-PTP did not affect the expression of endoglin, Flk-1, ICAM-2, N-cadherin, PECAM-1, Tie-2, or VE-cadherin.

should cause a truncation of the VE-PTP protein within the 16th fibronectin type III repeat of the extracellular domain, thus deleting the 17th fibronectin type III–like repeat, the transmembrane, and the catalytic domain of the phosphatase (Figure 1A). At the same time, this targeting strategy led to expression of nuclear β-galactosidase under the control of the endogenous *VE-PTP* promoter.

VE-PTP heterozygous mice were phenotypically indistinguishable from wild-type (wt) littermates concerning viability, fertility, and general appearance, whereas homozygous mutant embryos died at midgestation. Viability decreased between E8.5 and E9.5, resulting in the absence of viable homozygous mutant embryos at E10.0 (Table 1).

Table 1. VE-PTP genotype

Stage	No. of litters	No. of progeny				
		+/+	+/mt	mt/mt	Total	Viable mt/mt, no. (%)
E7.5-8.0	10	14	32	12	58	12 (100)
E8.5	44	44	83	36	163	26 (72)
E9.0	19	32	65	38	135	28 (73)
E9.5	35	53	113	62	228	32 (51)
E10.0	3	11	12	7	30	1 (3)
E10.5	7	8	28	17	53	0 (0)
E11.5	1	1	3	1	5	0 (0)
E12.5	6	16	22	13	51	0 (0)
E16.5	1	5	2	1	8	0 (0)
Total	126	184	360	187	731	99

Analysis of progeny from VE-PTP$^{+/mt}$ intercrosses.

To determine the nature of the mutated VE-PTP protein expressed from the targeted VE-PTP allele, polyoma middle-T-immortalized embryonic endothelial cells (e.Ends) were generated from VE-PTP wild-type, heterozygous, and homozygous mutant E9.5 embryos. In immunoprecipitations from lysates of ^{35}S-methionine–labeled wt e.Ends$^{+/+}$ using an mAb reactive with the VE-PTP ectodomain, VE-PTP was detected as the known 350-kDa/265-kDa doublet, whereas no VE-PTP species were detectable in the culture supernatant (Figure 1C). In contrast, a soluble form of VE-PTP was detected as a doublet of 275/205 kDa in culture supernatants of heterozygous and homozygous mutant cells (Figure 1C, lower panel), and the original 350-kDa/265-kDa membrane-spanning form of VE-PTP was detected only in lysates of heterozygous, but not of homozygous, mutant cells. Two additional lower-molecular-weight forms of VE-PTP (200 and 180 kDa) were detected in cell lysates of heterozygous and homozygous mutant cells. These nonsecreted forms as well as the secreted soluble forms were not recognized by antibodies against the C-terminus of VE-PTP (Figure 1B). We assume that the short 200/180-kDa forms are intracellular degradation products or differently modified forms of truncated VE-PTP. Of importance, no form of VE-PTP was found to be expressed on the cell surface of homozygous mutant endothelial cells by FACS analysis (Figure 1D). We conclude, that the gene disruption resulted in the loss of VE-PTP from the cell surface and the generation of a soluble secreted form of the protein lacking membrane anchoring and the intracellular phosphatase domain.

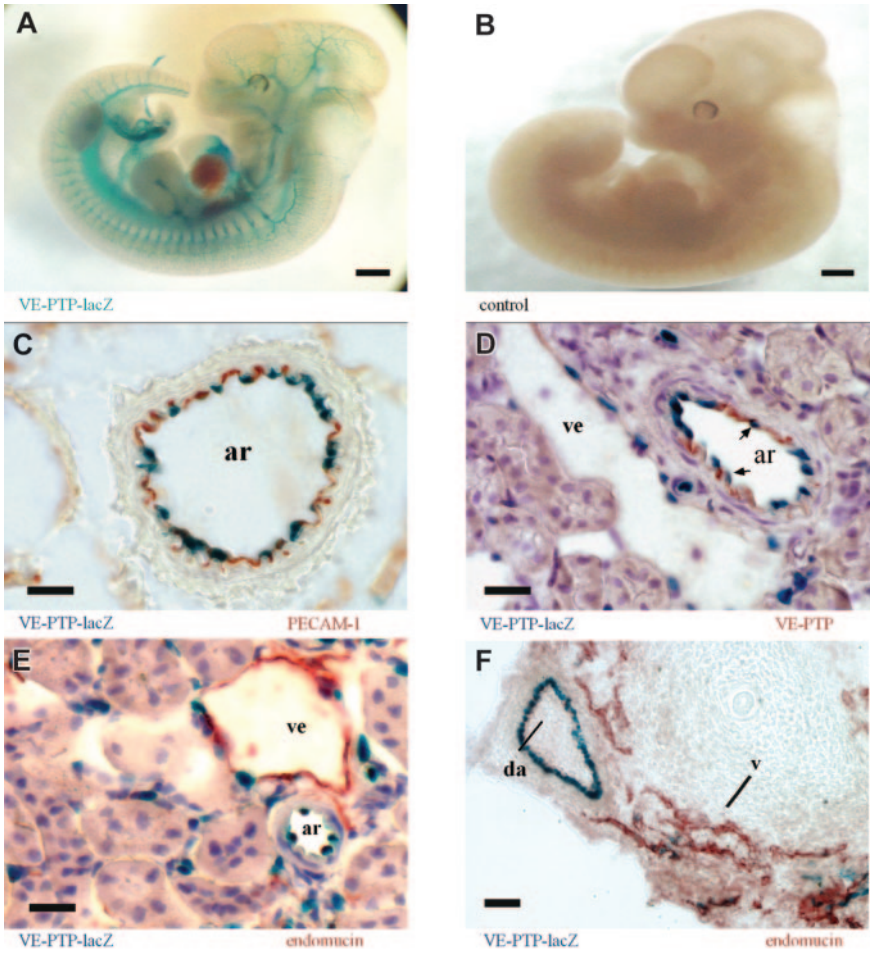

Figure 2. VE-PTP is predominantly expressed on arterial endothelium. (A) Whole-mount β-galactosidase staining of an E12.5 VE-PTP$^{+/mt}$ embryo showing a distinct vascular pattern of VE-PTP transcriptional activity (represented by the lacZ expression pattern), whereas the same staining of a wild-type littermate (B) was negative. (C-E) Cryosections of an adult VE-PTP$^{+/mt}$ heterozygous kidney. (C) An arterial vessel (ar) is immunolabeled for PECAM-1 (red) and endothelial nuclei are β-galactosidase stained (blue), recording VE-PTP transcriptional activity. (D) Immunolabeling for VE-PTP with mAb 109.3 (red) and β-galactosidase staining (arrows depict endothelial nuclei). Note that VE-PTP protein and transcriptional expression are more prominent in arterial endothelium (ar) than in venular endothelium (ve). (E) Immunolabeling for endomucin (red) stains predominantly venular endothelium (ve), whereas the β-galactosidase staining is more prominent in nuclei of arterial endothelium (ar). (F) Cryosection of an E12.5 VE-PTP$^{+/mt}$ embryo stained like sections in panel E. Note transcriptional activity of VE-PTP in the dorsal aorta (da, blue), but only weakly in neighboring venules (v), stained for endomucin (red). Bars represent 500 μm (A-B) and 20 μm. Objectives used: (A-B) Plan S 1 ×/0.085 numeric aperture (NA); (C-F) Plan Apochromat 20 ×/0.60 NA.

Surface expression of endoglin, VEGFR2/Flk-1, ICAM-2, N-cadherin, PECAM-1, Tie-2, and VE-cadherin, analyzed by flow cytometry (Figure 1D), was normal in homozygous mutant e.Ends.

VE-PTP is selectively expressed on endothelium and predominantly on arterial endothelium

Using the VE-PTP-lacZ knock-in allele as a means to monitor VE-PTP transcriptional activity, we examined the VE-PTP expression pattern during embryonic development as well as in various tissues from adult heterozygous mice. Whole-mount lacZ stainings of heterozygous embryos displayed a distinct vascular pattern of VE-PTP expression (Figure 2A). In order to analyze directly the expression pattern of the VE-PTP protein, we generated mAbs against mouse VE-PTP, using a VE-PTP-Fc fusion protein as immunogen. Analyzing cryosections of various adult organs of heterozygous mice revealed endothelial-specific expression by both β-galactosidase staining and immunohistochemistry (IHC) with the mAb 85.1 against VE-PTP (Figure S1, available on the *Blood* website; see the Supplemental Figures link at the top of the online article). VE-PTP could not be detected on mouse peripheral blood leukocytes by flow cytometry (not shown). As shown in Figure 2C, nuclear staining of β-galactosidase from VE-PTP promoter-driven lacZ expression colocalized with immunoperoxidase staining for PECAM-1 to the innermost cell layer of the depicted arteriole. However, VE-PTP expression varied among different subsets of endothelial cells along the vascular tree. Double staining for β-galactosidase and for the VE-PTP protein of adult kidney sections showed that arterial endothelium was stained much more strongly than venular endothelium by either method (Figure 2D). This was further substantiated by double staining for β-galactosidase and the sialomucin endomucin, which is highly enriched on venular endothelium. As shown for adult kidney sections (Figure 2E) and for sections of E12.5 heterozygous embryos (Figure 2F), the stainings for β-galactosidase and for endomucin were almost complementary, with strong arterial and only weak venular expression of lacZ. In summary, VE-PTP expression is restricted to the endothelial cell lineage with a remarkable preference for arterial endothelium (Table 2).

Targeted disruption of the VE-PTP gene leads to early embryonal vascular defects

Because VE-PTP homozygous mutant embryos died by E10, we analyzed embryonic phenotypes from E8.0 to E9.5. No phenotypic

Table 2. Relative expression levels on different vascular segments

	Arteries	Veins	Glomeruli
VE-PTP-IRES-lacZ	++	+	++
VE-PTP	++	+/−	++
Endomucin	−	++	+
PECAM-1	++	++	++

Semiquantitative analysis of the relative staining intensity of different types of blood vessels for the indicated antigens.

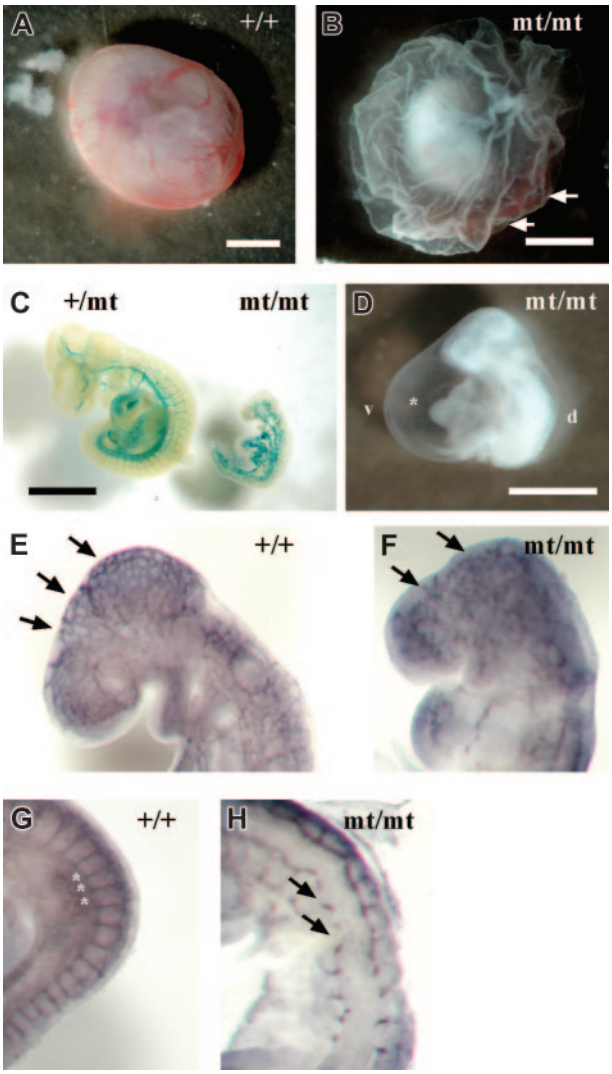

Figure 3. Developmental defects in VE-PTP-lacZ homozygous embryos. (A) Normal vascularization in an E9.5 wild-type yolk sac. (B) Pale yolk sac of a VE-PTP$^{mt/mt}$ embryo with blood islands (arrows). (C) Growth retardation in a rare E10.0 homozygous VE-PTP mutant, stained for β-galactosidase. The VE-PTP$^{+/mt}$ embryo on the left had 25 somite pairs, whereas its VE-PTP$^{mt/mt}$ littermate on the right was less than half the size and had only 10 somite pairs. (D) Pale-looking E9.5 VE-PTP homozygous mutant embryo with severely enlarged pericardium (asterisk). d indicates dorsal; v, ventral. (E-H) E9.0 embryos immunostained as whole mounts for PECAM-1. (E) Well-organized cerebral vascular network (arrows) in an E9.0 wild-type embryo brain. (F) Disconnected clusters of endothelial cells (arrows) in a VE-PTP$^{mt/mt}$ littermate. (G) Well-defined intersomitic sprouts (asterisks) in an E9.0 wild-type embryo, whereas intersomitic vessels (arrows) failed to develop in a homozygous mutant embryo (H). Bars represent 1 mm. A Plan S 1 ×/0.085 NA objective was used to visualize all images in these panels.

alterations were apparent prior to E8.5. However, at later developmental stages, homozygous mutant embryos were easily identifiable by their pale, fragile yolk sac lacking a directly visible hierarchically organized vascular network (Figure 3B). VE-PTP mutant embryos displayed a hugely dilated pericardial cavity, incomplete turning, and a pale gross appearance compared with their littermates (Figure 3D). During the period between E8.5 and E9.5, homozygous mutant embryos became progressively growth retarded (Figure 3C). Whole-mount PECAM-1 staining of E9.0 embryos revealed a disorganized vascular pattern in homozygous mutant embryos compared with wild-type embryos (Figure 3E-F). Intersomitic vessels in E9.0 homozygous embryos were stunted or even completely absent (Figure 3H).

The vascular defects prompted us to examine expression levels of several factors and receptors known to be relevant for angiogenesis. Expression levels were analyzed by reverse-transcriptase (RT)–PCR with RNA preparations from E9.5 wt and homozygous mutant embryos. No differences were detected for the tyrosine kinase receptors *Tie-1*, *Tie-2*, *VEGF-R1*, *VEGF-R2*, *EphB2*, *Eph B3*, *Eph B4*, and ephrin B2 and the soluble factors *Ang1*, *Ang2*, and *VEGF-A* (Figure S2). Since the vascular system of E9.5 mutant embryos was distorted, embryos were examined for signs of apoptosis of endothelial cells. Neither TUNEL staining nor staining for caspase 3, nor ultrastructural analysis of ultrathin sections of these embryos, allowed for the detection of endothelial apoptosis beyond the low level commonly detected in wt embryos (not shown).

VE-PTP gene disruption causes defects in embryonic heart formation

Comparative analysis of heart regions from PECAM-1 whole-mount immunolabeled embryos showed distinct differences in development between E9.5 homozygous mutant and normal embryos (Figure 4A-B). In wild-type embryos, the ventricular wall was covered by the intricately branched endocardium indicative of the ongoing trabecularization. In homozygous mutant embryos, the endocardial tube lacked the normal arborization (Figure 4B), suggesting a defective or delayed trabeculation.

Heart sections of E9.5 embryos were analyzed by double staining for N-cadherin and VE-cadherin. Whereas the N-cadherin–positive myocardial wall of wt embryos showed numerous attachment points to the VE-cadherin–positive endocardium, accompanied by first signs of myocardial trabeculation (Figure 4C), the endocardium in homozygous mutant littermates failed to attach to the myocardium, indicating defects in the process of trabeculation (Figure 4D).

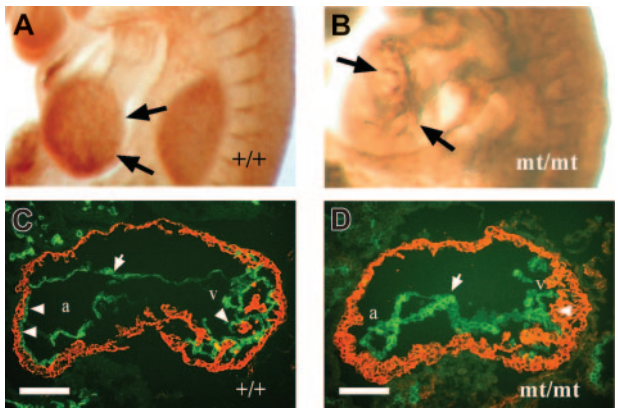

Figure 4. Abnormal heart development in VE-PTP mutant embryos. (A-B) E9.5 embryos immunostained as whole mounts for PECAM-1 show normal trabeculation (arrows) in wild-type hearts (A), and impaired ventricular trabeculation (arrows) in VE-PTP mutant hearts (B). (C-D) Cryosections through the heart regions of E9.5 wt (C) and VE-PTP homozygous mutant embryos (D). The myocardium was stained for N-cadherin (red) and the endocardium (arrow) for VE-cadherin (green). Whereas multiple attachment points between endocardium and myocardium are apparent in the atria of wt hearts (a) and trabeculation has started in the ventricular region (v) marked by arrowheads, the heart of mutant embryos showed alterations in endocardial cell morphology and failure of the endocardium to attach to the myocardium. Note the impaired myocardial trabeculation (arrowhead on the right). a indicates atrium of the heart; v, ventricle of the heart. Bars represent 100 μm. Objectives used: (A-B) Plan S 1 ×/0.085 NA; (C-D) Fluar 20 ×/0.75 NA.

VE-PTP mutant extraembryonic tissues display defective vascular remodeling

The pale yolk sacs of homozygous mutant embryos prompted us to directly examine the existence of a vascular network by staining for endothelial PECAM-1. Yolk sacs of mutant and wt embryos were stained and subsequently mounted on glass slides. As shown in Figure 5A-B, vascularization of yolk sacs of E8.5 mutant embryos appeared largely similar to that of wt embryos except for some tendency to slightly enlarged vessels in the mutants. However, yolk sacs of E9.5 mutant embryos displayed large areas containing uninterrupted layers of PECAM-1–positive endothelial cells instead of a well-structured hierarchic organization of blood vessels of different calibers typical for the wt yolk sacs (Figure 5C-D).

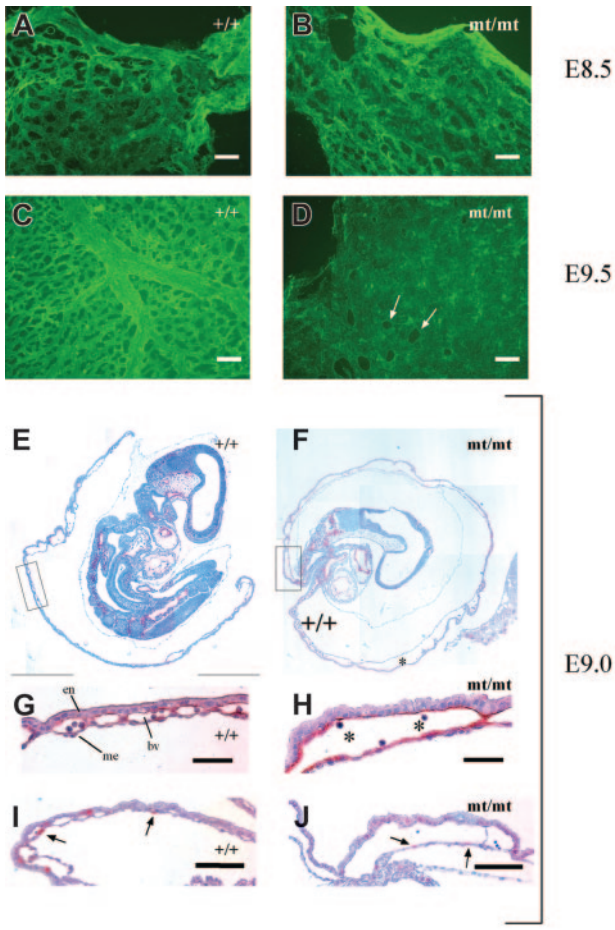

Figure 5. Vascularization defects in VE-PTP mutant yolk sac. (A-D) Yolk sacs of E8.5 and E9.5 wt and mt/mt embryos (as indicated) were stained by indirect immunofluorescence for PECAM-1 and mounted on poly-L-lysine–coated glass slides. Whereas the vessel network in the mt/mt yolk sacs of E8.5 embryos (B) consisted of a rather normal honeycomb-like vascular plexus, the E9.5 mt/mt yolk sac (D) contained enormous continuous layers of endothelium, in contrast to the well-developed hierarchic organization of large and small vessels in the wt yolk sac (C). Arrows in panel D mark endothelium-free areas. (E-F) Paraffin sections of E9.0 wt and mt/mt yolk sacs still containing the embryo proper were immunostained for endomucin. Note the dramatically enlarged vessels in the mt/mt yolk sac (asterisk). The boxed areas in panels E and F are shown at higher magnifications in panels G and H. en indicates endoderm; me, mesothelium; and bv, blood vessel. Asterisks indicate blood cells. (I-J) Paraffin sections of the yolks sacs of E9.0 wt and mt/mt embryos were stained for the proliferation marker phosphohistone-3. Arrows depict nuclei in endothelial cells. Bars represent 50 μm (A-D,G-H) and 100 μm (I-J). Objectives used: (A-D) Fluar 20 ×/0.75 NA; (E-F) Plan Apochromat 10 ×/0.45 NA; (G-J) Plan Apochromat 20 ×/0.60 NA.

This was further analyzed by staining sections of E9.0 yolk sacs for the endothelial marker endomucin. As shown in Figure 5E and 5G, wt yolk sacs contained normal blood vessels of various diameters embedded within the layers of extraembryonic endoderm and mesothelium.

In contrast, mutant yolk sacs showed a defective vasculature, consisting of dramatically increased cavities between the extraembryonic endoderm and mesothelium, lined by endothelium (Figure 5F,H). The formation of these large structures did not seem to be driven by a pathologic increase of endothelial proliferation since staining with an anti–phosphohistone-3 antibody (Figure 5I-J) detected 7% ± 4% positive endothelial nuclei in mutant yolk sacs and 6% ± 2% positive nuclei in wt specimens. Ultrastructural analysis of E9.5 homozygous mutant yolk sacs revealed that despite the unusual enlargement of the blood vessels, the contacts between endothelial cells showed no morphologic alterations (Figure S3). Tight junctions were still detectable. Thus, the lack of VE-PTP activity seems to affect the dynamics and the remodeling of blood vessels without causing major structural defects at cell contacts, as apparent from the ultrastructural analysis.

To further assess the role of VE-PTP in vascular morphogenesis, we turned to the allantois explant culture model. At E8.3, the cylinder-shaped allantoic sac usually contains a clearly stainable vascular network.[25] We prepared allantoides from E8.5 wild-type and VE-PTP mutant embryos and cultured explants on glass slides. Allantois explants from wt embryos attached to the substratum within 8 to 12 hours and were analyzed 22 hours after plating, when they had formed a disklike structure consisting of mesenchymal cells, containing a well-organized network of endothelial cells that stained positive for VE-cadherin (Figure 6A). The corresponding explants of homozygous VE-PTP mutants contained rather large VE-cadherin–positive cellular areas that did not resemble the filigran meshwork seen in wt explants (compare Figure 6A and 6B). The same result was obtained by staining for PECAM-1 (Figure 7A-B). Computer-assisted quantification of PECAM-1–stained explants revealed that the fraction of the tissue area covered by endothelial cells was 39% ± 8.7% larger in VE-PTP$^{mt/mt}$ than in wt/heterozygous allantoides (Figure 6I). For comparison, we analyzed allantois explants of Flk-1$^{-/-}$ and of Tie-2$^{-/-}$ embryos. Whereas no endothelial structures were detectable in Flk-1$^{-/-}$ allantoides, Tie-2$^{-/-}$ explants showed a perfectly normal vascular network (Figure 6C-F). In contrast, wt allantois explants that were cultured in the presence of a VE-cadherin blocking mAb lost the endothelial meshwork completely, confirming results by others.[8] Thus, the VE-PTP mutation affects the vascular structures in allantois explants differently than the lack of Flk-1 and Tie-2 or the blocking of VE-cadherin function.

To understand more about the way VE-PTP affects the formation of blood vessels in allantois explants, we observed the endothelial structures in homozygous VE-PTP mutant explants at higher magnification. We detected networks of endothelial cords in the mutant explants containing cords of similar thickness as seen for those in wt explants, yet the space between these cords was often filled with additional PECAM-1–positive cells (Figure 7B). PECAM-1 staining of these areas between endothelial cords was weaker, suggesting that these endothelial areas might be thinner than the cords (Figure 7B). This prompted the idea that the areas between cords contained endothelial cells that grew as simple endothelial monolayers. Indeed, laser scanning confocal microscopy revealed that endothelial cells in wt allantois explants usually

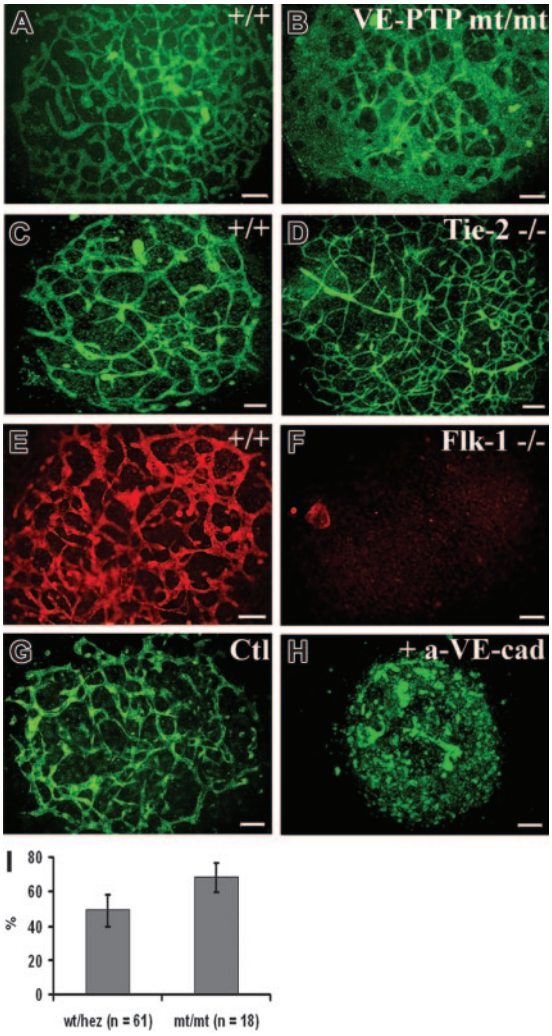

Figure 6. Explants of homozygous VE-PTP mutant allantois fail to undergo normal vascular morphogenesis in culture. (A-H) E8.5 allantoides of embryos of the following genotypes were explanted and cultured for 22 hours: wt (A,C,E,G), VE-PTP homozygous mutant (B), Tie-2$^{-/-}$ (D), Flk-1$^{-/-}$ (F), and wt (H); the latter was treated with blocking antibody against VE-cadherin. The vascular network was stained by indirect immunofluorescence either for VE-cadherin (A-F) or for PECAM-1 (G-H). Note that the VE-PTP mt/mt allantois displayed a reduction in the amount of avascular space and contained unusually large areas covered with endothelial cells. In contrast, wt and Tie-2$^{-/-}$ allantoides contained normal filigran networks of endothelial cords. As expected, no cordlike vascular structures were detected in the Flk-1$^{-/-}$ allantois. The allantois shown in panel H was cultured in the presence of an adhesion-blocking antibody against VE-cadherin, causing a complete disruption of vascular structures, while no such effect was seen in the control (G) treated with an isotype-matched control mAb. Bars represent 100 μm. (I) Percentage of surface area (±SD) stained for PECAM-1 in E8.5 wt/heterozygous and VE-PTP$^{mt/mt}$ cultured allantoides explants, with the total area of each explant set at 100%. The fraction of PECAM-1–positive areas was 39% ± 8.7% larger in VE-PTP$^{mt/mt}$ than in wt/heterozygous allantoides ($P < .01$). An HC Plan Apochromat 20 ×/0.70 NA objective was used to visualize all images in these panels.

displayed a complex multilayered cellular architecture (Figure 7C,E). While such structures were also detected in mutant explants (not shown), areas between these structures contained much simpler monolayer-like endothelial cell arrangements (Figure 7D,F). Since we found that freshly isolated allantoides of mutant E8.5 embryos contained a proper vascular network (not shown), and since initial blood vessels are generally formed within the rest of the embryo (Figure 3), we conclude that VE-PTP function is not necessary for the initial formation of blood vessels, but for their maintenance.

Discussion

VE-PTP is the first known receptor-type phosphotyrosine phosphatase that is restricted to endothelial cells. This was first shown by in situ hybridization analysis of embryonic tissue sections[12] and is confirmed here for the VE-PTP protein by immunohistochemistry for embryonic and adult tissues. The immunostainings shown here allowed us to determine unequivocally that VE-PTP is expressed on endothelial cells and not on perivascular cells. This endothelial specificity in combination with the previously described physical association of VE-PTP with Tie-2 and VE-cadherin, 2 essential cell-surface proteins for the development of the vascular system, raised the question whether VE-PTP might be involved in blood vessel formation. Our analysis of mice expressing a mutated form of VE-PTP, lacking its phosphatase domain as well as its ability to be membrane anchored, has revealed that the activity of VE-PTP is indeed essential for angiogenesis. Whereas de novo blood vessel formation (vasculogenesis) was clearly observed in homozygous mutant mice, the intraembryonic vasculature deteriorated at mid-gestation, and vessels in extraembryonic tissue such as the yolk sac showed dramatic defects in remodeling, resulting in huge blood cavities lined by endothelium. This establishes VE-PTP as a novel essential player in blood vessel remodeling and angiogenesis.

The dramatically enlarged vessels in the yolk sacs of E9.5 homozygous mutant mice developed from an originally normal vascular plexus, as judged by immunofluorescence of embryo sections of earlier stages. Changes in endothelial cell proliferation as a potential reason for this anomaly could be excluded since the

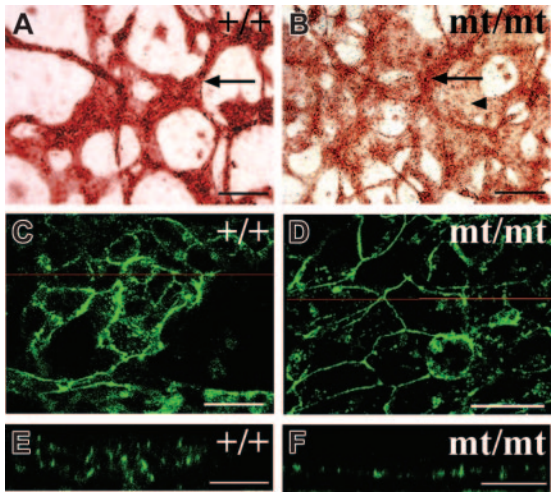

Figure 7. Endothelial cells grow as cell layers in cultured VE-PTP homozygous mutant allantoides. Allantoides were isolated from E8.5 wt (A,C,E) and VE-PTP mt/mt embryos (B,D,F) and cultured as explants for 22 hours. In panels A-B, they were stained by indirect immunoperoxidase staining for PECAM-1; in panels C-F, by indirect immunofluorescence for VE-cadherin. In panel B, note that the additional area covered by PECAM-1–positive endothelial cells (marked by an arrowhead) is less strongly stained than the cordlike structures (marked by an arrow), appearing to be "thinner" than the cords. Such a "thin" area stained for VE-cadherin is shown in panel D and compared with cordlike endothelial structures in panel C. The z-scans shown in panels E and F are taken from the micrographs in panels C and D, respectively, taken at the position of the red line. Note that the endothelium in the z-scan of the wt allantois showed a multilayered organization (E), whereas the endothelium in the mt/mt allantois appeared to be a single cell layer (F). Single endothelial cell layers ranged from 5- to 6-μm thickness in 10 analyzed areas, whereas the thickness of endothelial cord structures in mt allantoides was 16 to 20 μm (5 cords determined) and in wt allantoides 22.1 ± 7 μm (19 cords determined). Bars represent 100 μm (A-B) and 25 μm (C-F). Objectives used: (A-B) Plan Apochromat 20 ×/0.60 NA; (C-F) HC Plan Apochromat 20 ×/0.70 NA.

number of endothelial nuclei stained by an anti–phosphohistone-3 antibody was similar for mutant and wt embryos. Thus, the observed changes in vessel morphology are probably based on mechanisms that affect vessel remodeling. One possible explanation would be the lack of intussusception of growing blood vessels.[26] While this would indeed be a mechanism that would lead to enlarged vessels, it would not fully explain the extent of vessel enlargement we observed. Since the number of attached areas between extraembryonic endoderm and mesothelium, filling the gaps between blood vessels, was clearly reduced in mutant yolk sacs, the enlarged vessels did not just represent larger pre-existing vessels, but rather a smaller number of vessels that must have formed, at least partially, by fusion of smaller pre-existing vessels. The driving force for this is yet unclear. Another possible explanation for vessel enlargement would be VEGF-mediated hyperfusion.[27] Indeed, DEP-1 mutant mouse embryos showed clear signs of vessel enlargement in yolk sacs and had 5- to 10-fold increased levels of VEGF transcripts.[11] However, this mechanism can be excluded for our VE-PTP mutants, since we did not detect any changes of VEGF transcript levels. An attractive hypothesis for the development of enlarged vessels in VE-PTP mutants would be that interendothelial cell contacts or sites of attachment between the endothelium and mesothelial or endodermal cells, respectively, might become weakened by the lack of VE-PTP activity. This could facilitate changes in vessel size and morphology in mutant embryos. Since we have found recently that VE-PTP can indeed support the adhesive function of VE-cadherin in transfected cells,[14] and the inhibition of VE-PTP expression by small-interfering RNA reduces VE-cadherin function in endothelial cells (A.G., A.H., Giuseppe Cagna, Mark Winderlich, Stephan Kloep, Stefan Butz, and D.V., manuscript in preparation), destabilizing effects on endothelial cell contacts would be expected in the homozygous VE-PTP mutants analyzed here. Ultrastructural analysis (Figure S3), however, still revealed intact tight junctions at interendothelial cell contacts in yolk sacs of mutant embryos. Thus, a destabilizing effect on endothelial cell contacts potentially caused by the absence of VE-PTP would have to be more subtle, possibly causing a higher plasticity and increased dynamics of contact stability allowing pathologic fusion of blood vessels.

Freshly isolated E8.5 allantoides of homozygous mutant embryos contained a vascular network similar to those of wt embryos (not shown). When these allantoides were cultured for 22 hours, only the mutant explants showed an outgrowth of monolayer-like endothelial cell arrangements extending from existing endothelial cords. Again, this shows that endothelial cords were initially formed, but endothelial cells did not remain in these structures and seemed to be able to dissociate and grow out as an endothelial layer, a process probably furthered by the 2-dimensional growth conditions of the explant cultures lacking any blood flow. As mentioned, an attractive hypothesis to explain this outgrowth phenomenon would be the potential weakening of interendothelial cell contacts caused by the lack of VE-PTP. The alternative possibility that the endothelial monolayers were formed by mesodermally derived angioblasts recruited to the cords is less likely, but cannot be ruled out.

Since Tie-2 is a substrate and association partner of VE-PTP, this tyrosine kinase is another obvious candidate molecule to be involved in the mechanisms that lead to the VE-PTP mutant phenotype. Of interest, the vascular network of E9.5 yolk sacs of Tie-2$^{-/-}$ embryos has been reported to consist of dilated vessels,[28] reminiscent of what we observed for yolk sac vessels in the VE-PTP mutant embryos. However, vessel enlargement in the Tie-2$^{-/-}$ mice is much milder. Furthermore, we show here that the vascularization of cultured E8.5 explants of Tie-2$^{-/-}$ allantoides was normal and undistinguishable from the wild-type situation. Thus, although it is conceivable that the lack of VE-PTP activity may affect Tie-2–mediated functions, it is unlikely that the much more dramatic defects we have observed here for VE-PTP mutant embryos are merely a consequence of compromised Tie-2 functions.

VE-cadherin, the second protein known to be associated with VE-PTP, is a more likely candidate for being involved in the mechanisms that lead to the vascular defects in VE-PTP mutant mice. As described, we have found that VE-PTP supports the adhesive function of VE-cadherin in endothelial cells. In agreement with this, VE-cadherin$^{-/-}$ embryos were found to die at a similar time between E9.5 and E10.0[6] as do the VE-PTP mutant embryos; although in a separate study, lethality of independently established VE-cadherin$^{-/-}$ embryos was determined to occur as late as E11.5.[7] Initial formation of blood vessels and of interendothelial cell contacts and junctions was clearly detected in both studies. The yolk sacs of E9.0 VE-cadherin–null embryos were reported to lack proper vessel assembly[7] or contained blood vessels that progressively disconnected from each other at branches, thereby inducing stagnating blood lakes.[6] Explants of E8.5 VE-cadherin$^{-/-}$ allantoides cultured for 18 hours were devoid of a capillary plexus,[8] whereas the effect we observed in allantois explants of VE-PTP mutants was milder, leading only to the planar outgrowth of endothelial cells from cord structures without the complete loss of the cord network. Taken together, it is conceivable that the VE-PTP$^{mt/mt}$ phenotype could partially be based on reduced VE-cadherin adhesion activity. The additional effect of induced endothelial apoptosis caused by VE-cadherin deficiency[6] could not be observed in VE-PTP mutant embryos, suggesting that VE-PTP is not involved in the signaling events by which VE-cadherin inhibits apoptosis.

Other RPTPs expressed in endothelial cells, although not exclusively, are RPTPμ and the density-enhanced phosphatase 1 (DEP-1, CD148). RPTPμ was even reported to directly associate with VE-cadherin via their cytoplasmic domains and to support VE-cadherin's adhesive function.[29] Disruption of the RPTPμ gene, however, did not impair angiogenesis and embryonic development.[30] In contrast, mice homozygous for a mutant *DEP-1* allele, in which the phosphatase domain of DEP-1 was eliminated by an in-frame replacement with enhanced green fluorescent protein (EGFP), are embryonic lethal and die before E11.5.[11] Besides growth retardation and both intraembryonic and extraembryonic vascular anomalies, increased proliferation and expansion of the endothelial cell compartment were observed, consistent with reported growth-inhibitory functions of DEP-1.[31-33] Of interest, the vasculature in yolk sacs of E9.5 to E10.5 DEP-1 mutants showed clear signs of enlargements, although the effect was less dramatic than the defects we observed in our VE-PTP mutants. Since DEP-1 is not an endothelial-specific protein, it is not known whether vessel enlargement is indeed an endothelial defect or whether the DEP-1 mutation might affect the separation of the endoderm and mesothelial cell layers. This cell layer separation was also caused by gene deficiencies for 2 adhesion molecules, namely N-cadherin[34] and the integrin chain α_5.[35] In both cases, these defects resulted in enlarged blood-filled cavities within the yolk sac.

It is interesting that VE-PTP was not found evenly distributed among different types of blood vessels with a much more pronounced expression in arterial versus venular vessels. Despite their different requirements for embryonic development, the same was reported for RPTPμ.[30] Whether this arterial preference of VE-PTP and RPTPμ expression reflects differences in endothelial

cell contact stability between arterial, capillary, and venous endothelium[36,37] that could be caused by dephosphorylation of junctional molecules will have to be analyzed in the future.

In addition to the vascular defects, we have observed anomalies in heart development with respect to a defective or delayed trabeculation, a lack of association between endocardium and myocardium, and a dilated pericardial cavity. It has been reported that the development of the embryo is critically dependent on the formation and maintenance of a functioning yolk sac circulation. Lack of this circulation results in growth retardation and swelling of the pericardium, which is often an indicator of osmotic imbalances within the embryo.[38] It is unclear what causes the lack of attachment between endocardium and myocardium. It is possible that this may simply be a consequence of a delayed development. Alternatively, this may hint at further functions of VE-PTP in the endocardium that go beyond the maintenance and stability of vessel structures.

In summary, our results suggest that VE-PTP is critically involved in the maintenance of vascular structures during embryonic development, as was most prominently visible in the extraembryonic vasculature. The association with VE-cadherin and the support of VE-cadherin function by VE-PTP in combination with the fact that VE-cadherin is essential for the maintenance of blood vessels suggest that at least some of the essential functions of VE-PTP in blood vessel formation and embryonic development may be exerted via VE-cadherin.

Acknowledgments

We thank Dr Friedemann Kiefer for advice with the establishment of endothelioma cell lines, Dr Valentin Djonov for discussions, Dr Achim Gossler for advice with preparing allantois explants, Silvia Hennig for expert technical assistance, and Dr Nicole Bäumer for her critical reading of the manuscript.

References

1. Risau W. Mechanisms of angiogenesis. Nature. 1997;386:671-674.
2. Gale NW, Yancopoulos GD. Growth factors acting via endothelial cell-specific receptor tyrosine kinases: VEGFs, angiopoietins, and ephrins in vascular development. Genes Dev. 1999;13:1055-1066.
3. Carmeliet P. Angiogenesis in health and disease. Nat Med. 2003;9:653-660.
4. Jain RK. Molecular regulation of vessel maturation. Nat Med. 2003;9:685-693.
5. Ferrara N, Gerber H-P, LeCouter J. The biology of VEGF and its receptors. Nat Med. 2003;9:669-676.
6. Carmeliet P, Lampugnani M-G, Moons L, et al. Targeted deficiency or cytosolic truncation of the VE-cadherin gene in mice impairs VEGF-mediated endothelial survival and angiogenesis. Cell. 1999; 98:147-157.
7. Gory-Faure S, Prandini MH, Pointu H, et al. Role of vascular endothelial-cadherin in vascular morphogenesis. Development. 1999;126:2093-2102.
8. Crosby CV, Fleming PA, Argraves WS, et al. VE-cadherin is not required for the formation of nascent blood vessels but acts to prevent their disassembly. Blood. 2005;105:2771-2776.
9. den Hertog J, Blanchetot C, Buist A, Overvoorde J, van der Sar A, Tertoolen LG. Receptor protein-tyrosine phosphatase signalling in development. Int J Dev Biol. 1999;43:723-733.
10. Koop EA, Gebbink MF, Sweeney TE, et al. Impaired flow-induced dilation in mesenteric resistance arteries from receptor protein tyrosine phosphatase-mu-deficient mice. Am J Physiol Heart Circ Physiol. 2005;288:H1218-H1223.
11. Takahashi T, Takahashi K, St John PL, et al. A mutant receptor tyrosine phosphatase, CD148, causes defects in vascular development. Mol Cell Biol. 2003;23:1817-1831.
12. Fachinger G, Deutsch U, Risau W. Functional interaction of vascular endothelial-protein-tyrosine phosphatase with the angiopoietin receptor Tie-2. Oncogene. 1999;18:5948-5953.
13. Krueger NX, Streuli M, Saito H. Structural diversity and evolution of human receptor-like protein tyrosine phosphatases. EMBO J. 1990;9:3241-3252.
14. Nawroth R, Poell G, Ranft A, et al. VE-PTP and VE-cadherin ectodomains interact to facilitate regulation of phosphorylation and cell contacts. EMBO J. 2002;21:4885-4895.
15. Shalaby F, Rossant J, Yamaguchi TP, et al. Failure of blood-island formation and vasculogenesis in Flk-1-deficient mice. Nature. 1995;376:62-66.
16. Dumont DJ, Gradwohl G, Fong GH, et al. Dominant-negative and targeted null mutations in the endothelial receptor tyrosine kinase, tek, reveal a critical role in vasculogenesis of the embryo. Genes Dev. 1994;8:1897-1909.
17. Reiss Y, Kiefer F. Immortalization of endothelial cells. In: Augustin HG, ed. Methods in Endothelial Cell Biology. Berlin: Springer; 2004:63-72.
18. Gotsch U, Borges E, Bosse R, et al. VE-cadherin antibody accelerates neutrophil recruiment in vivo. J Cell Sci. 1997;110:583-588.
19. Koblizek TI, Runting AS, Stacker SA, Wilks AF, Risau W, Deutsch U. Tie2 receptor expression and phosphorylation in cultured cells and mouse tissues. Eur J Biochem. 1997;244:774-779.
20. Kataoka H, Takakura N, Nishikawa S, et al. Expressions of PDGF receptor alpha, c-Kit and Flk1 genes clustering in mouse chromosome 5 define distinct subsets of nascent mesodermal cells. Dev Growth Differ. 1997;39:729-740.
21. Morgan SM, Samulowitz U, Darley L, Simmons DL, Vestweber D. Biochemical characterization and molecular cloning of a novel endothelial specific sialomucin. Blood. 1999;93:165-175.
22. Bosse R, Vestweber D. Only simultaneous blocking of L- and P-selectin completely inhibits neutrophil migration into mouse petritoneum. Eur J Immunol. 1994;24:3019-3024.
23. Hahne M, Jäger U, Isenmann S, Hallmann R, Vestweber D. Five TNF-inducible cell adhesion mechanisms on the surface of mouse endothelioma cells mediate the binding of leukocytes. J Cell Biol. 1993;121:655-664.
24. Dorner AA, Wegmann F, Butz S, et al. Coxsackievirus-adenovirus receptor (CAR) is essential for early embryonic cardiac development. J Cell Sci. 2005;118:3509-3521.
25. Drake CJ, Fleming PA. Vasculogenesis in the day 6.5 to 9.5 mouse embryo. Blood. 2000;95:1671-1679.
26. Djonov V, Baum O, Burri PH. Vascular remodeling by intussusceptive angiogenesis. Cell Tissue Res. 2003;314:107-117.
27. Drake CJ, Little CD. Exogenous vascular endothelial growth factor induces malformed and hyperfused vessels during embryonic neovascularization. Proc Natl Acad Sci U S A. 1995;92:7657-7661.
28. Sato TN, Tozawa Y, Deutsch U, et al. Distinct roles of the receptor tyrosine kinases Tie-1 and Tie-2 in blood vessel formation. Nature. 1995; 376:70-74.
29. Sui XF, Kiser TD, Hyun SW, et al. Receptor protein tyrosine phosphatase microregulates the paracellular pathway in human lung microvascular endothelia. Am J Pathol. 2005;166:1247-1258.
30. Koop EA, Lopes SM, Feiken E, et al. Receptor protein tyrosine phosphatase mu expression as a marker for endothelial cell heterogeneity: analysis of RPTPmu gene expression using LacZ knock-in mice. Int J Dev Biol. 2003;47:345-354.
31. Keane MM, Lowrey GA, Ettenberg SA, Dayton MA, Lipkowitz S. The protein tyrosine phosphatase DEP-1 is induced during differentiation and inhibits growth of breast cancer cells. Cancer Res. 1996;56:4236-4243.
32. Trapasso F, Iuliano R, Boccia A, et al. Rat protein tyrosine phosphatase eta suppresses the neoplastic phenotype of retrovirally transformed thyroid cells through the stabilization of p27(Kip1). Mol Cell Biol. 2000;20:9236-9246.
33. Lampugnani MG, Zanetti A, Corada M, et al. Contact inhibition of VEGF-induced proliferation requires vascular endothelial cadherin, beta-catenin, and the phosphatase DEP-1/CD148. J Cell Biol. 2003;161:793-804.
34. Radice GL, Rayburn H, Matsunami H, Knudsen KA, Takeichi M, Hynes RO. Developmental defects in mouse embryos lacking N-cadherin. Dev Biol. 1997;181:64-78.
35. Yang JT, Rayburn H, Hynes RO. Embryonic mesodermal defects in α5 integrin-deficient mice. Development. 1993;119:1093-1105.
36. Majno G, Palade GE, Schoefl GI. Studies on inflammation, II: the site of action of histamine and serotonin along the vascular tree: a topographic study. J Biophys Biochem Cytol. 1961;11:607-626.
37. Horan KL, Adamski SW, Ayele W, Langone JJ, Grega GJ. Evidence that prolonged histamine suffusions produce transient increases in vascular permeability subsequent to the formation of venular macromolecular leakage sites: proof of the Majno-Palade hypothesis. Am J Pathol. 1986; 123:570-576.
38. Copp AJ. Death before birth: clues from gene knockouts and mutations. Trends Genet. 1995; 11:87-93.